"Improvement of mechanical and thermal properties of poly(3-hydroxybutyrate) (PHB) blends with surface-modified halloysite nanotubes (HNT)"

Daniel Garcia-Garcia[a]*, David Garcia-Sanoguera[a], Vicent Fombuena[a], Juan Lopez-Martinez[a], Rafael Balart[a].

[a] *Instituto de Tecnología de Materiales-ITM*

Universitat Politècnica de València

Plaza Ferrandiz y Carbonell 1, 03801, Alcoy, Alicante (Spain)

* Corresponding author: D. Garcia-Garcia

E-mail: dagarga4@epsa.upv.es

Tel.: (+34) 96 652 84 34

Fax: (+34) 96 652 84 33

ABSTRACT

The effect of two hydrophobic treatments on the hydrophilic nature of halloysite nanotubes (HNT) was studied in this research work: a silanization with (3-glycidyloxypropyl) trimethoxysilane (GLYMO) and a surface treatment with a natural aromatic compound, *i.e.* caffeic acid (CA). In addition, the effect of 3 wt% of unmodified HNT, silanized HNT (HNT_{SIL}) and caffeic acid-modified HNT (HNT_{CA}) on mechanical, thermal and morphological properties of a binary blend of poly(3-hydroxybutyrate) (PHB) and poly(ε-caprolactone) (PCL) with a weight ratio of 75/25, respectively was evaluated. These blends and their corresponding composites with HNT were partially compatibilized by reactive extrusion with dicumyl peroxide (DCP) and further processed by injection molding. The effectiveness of the surface treatments on HNT was followed by Fourier transformed infrared spectroscopy (FTIT), thermogravimetric analysis (TGA), field emission scanning electron microscopy (FESEM) and contact angle measurements. The obtained results suggested a clear hydrophobizing effect of both surface treatments on HNT but the hydrophobic nature the caffeic acid treatment can provide to HNT is greater than silanization. FESEM study on HNT-loaded PHB/PCL blends showed increased compatibility between modified-HNT and the polymeric matrix, as well as a better particle dispersion. In particular, 3 wt% HNT_{CA} lead to an increase in tensile strength and elongation at break of 11.4% and 74%, respectively, with regard to composites with unmodified HNT. In addition, thermal analysis, evaluated by differential scanning calorimetry (DSC) and thermogravimetric analysis (TGA), revealed a decrease in the melt peak temperature of 6.5ºC for composites with 3 wt% HNT_{CA} as well a delay in the onset degradation temperature, thus leading to a broader processing window which enhances PHB processing by conventional techniques.

Keywords: Poly(3-hydroxybutyrate); poly(ε-caprolactone); dicumyl peroxide; halloysite nanotubes; silane; caffeic acid.

1. INTRODUCTION

In the last years, important advances in the field of biodegradable polymers have been observed. Nevertheless, some of these polymers still show important drawbacks that restrict their wide use in industry. Poly(3-hydroxybutyrate) (PHB) is one of the most promising biopolyesters obtained from bacterial fermentation but it has to face an important challenge related to its fragility (due to its high crystallinity) and its extremely narrow processing window, since its thermal degradation is slightly higher than its melt process (Zhang and Thomas, 2010). These drawbacks, together with an still high price compared to commodity plastics are responsible for a very restricted industrial use (Godbole et al., 2003). To overcome or minimize these drawbacks, several approaches have been addressed in the last years with the main aim of increasing its thermo-mechanical performance. It is worthy to note the interesting results obtained by using natural-derived plasticizers such as epoxidized linseed oil (Garcia-Garcia et al., 2016), epoxidized soybean oil (Choi and Park, 2004) or maleinized linseed oil (Garcia-Garcia et al., 2017), among others. Another apporach has been physical blending with a wide variety of biodegradable polymers such as poly(lactic acid) (PLA) (Zhang and Thomas, 2011), poly(butylene succinate) (PBS) (Ma et al., 2012), poly(ε-caprolactone) (Gassner and Owen, 1994; Lovera et al., 2007) or poly(vinyl alcohol) (Azuma et al., 1992; Olkhov et al., 2003). Finally, the use of nanoparticles has been revealed as an interesting alternative to plasticizing and/or blending. It has been reported the positive effect of TiO_2 nanoparticles (Iulianelli et al., 2018), ZnO nanoparticles (Díez-Pascual and Díez-Vicente, 2014) or cellulose nanowiskers (S de O Patrício et al., 2013) on mechanical, thermal and barrier properties of PHB-based composites.

In our previous works, it was reported the positive effect of a binary blend of PHB and PCL with a weight ratio of 75/25 respectively, on overall thermal and mechanical ductile properties. Nevertheless, it was concluded that these two polyesters showed a highly restricted miscibility, leading to phase separation due to the poor interactions among PHB-PCL interface and this restricts the improvements PCL can provide (Garcia-Garcia et al., 2016). To overcome this, 1 phr dicumyl peroxide (DCP) was successfully used to promote reactive extrusion during blending, thus leading to a remarkable increase in ductile properties. In particular, the obtained elongation at break was increased by 231% with regard to the uncompatibilized PHB/PCL blend. Regarding the impact properties, the impact-absorbed energy (Charpy test) was improved by 91% thus giving clear evidences of the compatibilizing effect DCP provides, without compromising other mechanical resistant properties (Garcia-Garcia et al., 2017b).

The interest on ternary blends containing two polymers and one nanofiller is increasing due to the positive effect of nanoparticles on overall properties of blends. These nanoparticles provide a structural reinforcing role together with potential compatibilization. When two immiscible polymers are mixed together, there are not any interactions between the molecular segments of both polymers, which gives high surface tension between these polymers. This phenomenon is responsible for a poor dispersion of each polymer on the other, thus leading to phase separation with the typical drop-like structure (Taguet et al., 2014). Several authors have reported that the addition of small amounts of different nanofillers gives reduced surface tension between the two polymers thus lading to coalescence inhibition and a remarkable decrease in the particle size of the dispersed phase. This contributes to improved interface adhesion and gives improved compatibility to blends (Chen et al., 2015; Hemmati et al., 2014; Mofokeng and Luyt, 2015; Urquijo et al., 2017; Vrsaljko et al., 2015; Wu et al., 2011).

One of the most promising nanofillers in the last decade are halloysite nanotubes (HNT). These nanotubes are natural aluminosilicates with the molecular formula of $Al_2Si_2O_5(OH)_4 \cdot nH_2O$ (Lvov et al., 2008). HNT offer a hollow tubular structure composed of multiple layers of hollow cylinders with an elevated aspect ratio. An interesting feature of HNT is the different chemical structure of the outer surfaces with regard to the inner areas. The external (outer) surface is composed of siloxane (Si–O–Si) while the inner layers are composed of aluminol groups (Al–OH) (Jafarzadeh et al., 2015; Yuan et al., 2008). Furthermore, typical HNT show an inner diameter of 15 nm which allows using HNT as carriers for selective loads, thus allowing their use for controlled delivery systems (Kurczewska et al., 2018; Torres et al., 2017). All these features, together with a relatively low price make HNT high attractive as a functional additive in polymeric systems. Pal *et al.* (2014), studied the effect of the addition of 1 wt% unmodified halloysite and silanized halloysite with N-(β-aminoethyl)-γ-aminopropyltrimethoxysilane on overall properties of an immiscible blend between poly(oxymethylene) (POM) and poly(propylene) (PP). They reported an improvement on compatibilization and a slight increase in the thermal degradation onset. Nevertheless, one of the main drawbacks of a widespread use of HNT is their extremely high hydrophilicity, due to the presence of a huge number of hydroxyl groups which contributes to aggregate formation. This hydrophilicity contributes to poor dispersion with the subsequent negative effect on overall properties (Krishnaiah et al., 2017). To minimize these effects, during the last years, several research works have been focused on reducing the hydrophilicity of HNT, mainly by silanization surface treatments (Carli et al., 2014; Liu et al., 2008; Raman et al., 2013).

This work focuses on the use of a novel surface treatment with caffeic acid (CA). Caffeic acid is plant-derived aromatic compound which shows interesting properties such as antioxidant, anticancer, anti-inflammatory, antiviral activity, among others (Baykal et al., 2015). CA is used in this work with two main purposes. On one hand, its potential as surfactant material is studied with the aim of reducing hydrophilic properties of HNT and, on the other hand, its antioxidant potential to delay thermal degradation is addressed. A common silanization process with (3-glycidyloxypropyl) trimethoxysilane (GLYMO) is also carried out to compare the effects on the hydrophilic properties of HNT. Moreover, the effect of 3 wt% unmodified and modified (silanized and caffeic acid-modified) HNT on overall properties of a binary blend composed of PHB and PCL with a weight ratio of 75:25, respectively, partially compatibilized by reactive extrusion with dicumyl peroxide (DCP), is studied.

2. EXPERIMENTAL

2.1. Materials

Poly(3-hydroxybutyrate) (PHB) pellets commercial grade P304 were supplied by Biomer (Krailling, Germany). Poly(caprolactone) (PCL) (CAPA 6500, M_w = 50,000 Da) was provided by Perstorp Holding AB (Malmö, Sweden). Dicumyl peroxide (DCP) (98% purity), halloysite nanotubes (HNT), caffeic acid and the silane used for surface treatment of HNT ((3-glycidyloxypropyl) trimethoxysilane - GLYMO) were supplied from Sigma Aldrich (Madrid, Spain) and used without further purification. Acetic acid (99.7% CH_3COOH) was used as a mild acid to increase the lumen size in HNT. This was supplied by PanReac Applichem (Barcelona, Spain).

2.2. Silanization of HNT

Functionalization of HNT with silanes was carried out following the procedure described by Krishnaiah *et al.* (2017). Approx. 6 g silane (GLYMO) was dissolved in 250 mL ethanol (96%) and the solution was mechanically stirred for 15 min at 60ºC to hydrolyze alcoxy groups. Subsequently, acetic acid was added drop by drop until reaching a pH value around 5 and then, 25 g HNT were added while maintaining mechanical stirring at 60ºC for two additional hours. HNT were obtained by filtration and were washed with ethanol. Finally, silanized HNT were dried at 70ºC for 8 h with the aim of removing the residual moisture.

2.3. Acid treatment of HNT and caffeic acid loading.

Prior to load caffeic acid into HNT, the lumen diameter was selectively etched with acetic acid following the procedure described by Garcia-Garcia *et al.* (2017a) To this, HNT were previously dried at 100ºC for 8 h. Then 5 g dried HNT were poured into a 500 mL flask with an acetic acid solution in distilled water with a concentration of 1 mol L^{-1}. The solution was maintained with mechanical stirring for 72 h at 50ºC. After this treatment, chemically modified HNT were collected by centrifugation and washed with distilled water until a neutral pH was obtained. Finally, acid-treated HNT were dried at 50ºC for 24 h. After this surface treatment to increase the loading capacity, HNT were loaded with caffeic acid following the procedure described by Hendessi *et al.* (2016). A summary of this procedure is as follows: caffeic acid was dissolved in ethanol (96%) until saturation. Then, 5 g of HNT were poured to the solution. The suspension was sonicated for 5 min using an amplitude of 33% in an ultrasonic homogenizer Sonoplus HD 2200 from Bandelin (Berlin, Germany). After this, the mixture was subjected to vacuum (1 mbar) for 30 min to remove the trapped air inside HNT; then the vacuum was broken and the suspension remained at atmospheric pressure for 10 min to allow caffeic acid molecules to enter into the HNT lumen. The cycle was repeated 3 times to improve the loading efficiency. Finally, caffeic acid loaded HNT was separated by centrifugation at 4000 rpm for 5 min and washed with ethanol to remove the caffeic acid excess. Caffeic acid-loaded HNT were dried at 40ºC for 24 h.

2.4. Manufacturing of PHB/PCL blends with different HNT loads

PHB and HNT were dried in a vacuum oven at 70ºC for 8 hours while PCL was dried at 40ºC overnight to remove residual moisture before use. The appropriate amounts of PHB, PCL, DCP and 3 wt% unmodified HNT, silanized HNT (HNT_{SIL}) and caffeic acid-treated HNT (HNT_{CA}) were pre-mixed mechanically in a zipper bag prior to compounding. The compositions of PHB/PCL/DCP/HNT blends are listed in Table 1. All the samples were melt-blended in a co-rotating twin-screw extruder from DUPRA S.L. (Alicante, Spain) with a screw diameter of 25 mm and a length (L) to diameter (D) ratio, *i.e.* L/D, of 24. The screw speed was set to 40 rpm to allow reactive extrusion and the temperature profile of the extrusion barrel was set to 165ºC (hopper), 170ºC, 175ºC and 180ºC (extrusion die). The obtained compounds were cooled down to room temperature, pelletized and subsequently processed by injection moulding in a Meteor 270/75 from Mateu & Solé (Barcelona, Spain) to obtain standard samples for further characterization. The temperature profile for the injection process was set to 165ºC, 165ºC, 170ºC, 175ºC and 180ºC from feeding zone to the injection nozzle. The cavity filling and cooling times were set to 1 and 30 s, respectively. Prior to characterization, standard samples were stored at room conditions (23 ± 1°C and 50% HR) for 21 days with the main aim of stabilizing mechanical properties of the obtained blends since PHB undergoes physical aging due to crystallization with time. Previous results have reported that mechanical properties tend to stabilize after the above-mentioned aging time (Kurusu et al., 2014).

Coding	PHB (wt%)	PCL (wt%)	HNT (wt%)	DCP (phr)
PHB/PCL/DCP	75	25	0	1
3-HNT	72.75	24.25	3	1
3-HNT$_{SIL}$	72.75	24.25	3	1
3-HNT$_{CA}$	72.75	24.25	3	1

Table 1. Composition and labelling of binary PHB/PCL compatibilized by reactive extrusion with DCP and reinforced with unmodified and modified HNT.

2.5. Characterization techniques

2.5.1. Fourier Transformed Infrared Spectroscopy (FTIR)

The effect of the different treatments on the chemical structure of HNT was studied by Fourier transformed infrared spectroscopy in a FTIR spectrometer Spectrum BX from Perkin-Elmer (Madrid, Spain). HNT were subjected to 20 scans between 4000 and 400 cm^{-1} with a resolution of 16 cm^{-1}. Prior to sample characterization, 1.2 mg of each type of HNT were mechanically mixed with KBr until homogenization, and subsequently pressed to obtain the corresponding cylindrical discs (120 mg).

2.5.2. Field emission scanning electron microscopy and energy dispersive X-ray analysis (FESEM-EDS)

The effect of the different surface treatments on HNT, as well as the morphology of fractured blends from impact tests was studied in a field emission scanning electron microscope (FESEM) ZEISS model ULTRA 55 (Eindhoven, The Netherlands), equipped with an energy dispersive spectrometer (EDS). Image acquisition was carried out at an accelerating voltage of 5 kV. Prior to be observed fractured surfaces of samples were coated with a thin layer of platinum in a high vacuum sputter coater EM MED20 from Leica Microsystem (Milton Keynes, United Kingdom).

2.5.3. Dynamic contact angle measurements

The effect of the surface treatments of HNT on their wetting properties was analysed by optical goniometry in an Easy Drop Standard KRÜSS goniometer (KRÜSS GmbH, Hamburg, Germany), model FM140 (110/220 V, 50/60 Hz).

2.5.4. Mechanical properties

Tensile and flexural properties of PHB/PCL blends loaded with HNT were obtained using a universal test machine Ibertest ELIB 30 from SAE Ibertest (Madrid, Spain) according to ISO 527 and ISO 178 respectively. Both tests were carried out with a 5 kN load cell and a crosshead speed of 5 mm min^{-1}. Moreover, for a more accurate determination of the Young's modulus, an axial extensometer IB/MFQ-R2 from Ibertest (Madrid, Spain) coupled to the universal test machine was used. All specimens were tested at room temperature (23 ± 1 °C) and at least five samples for each material were analysed for each mechanical test and averaged values of the main mechanical parameters were calculated.

2.5.5. Thermal properties

The effect of loading HNT on thermal properties of the partially compatibilized PHB/PCL blend was studied by differential scanning calorimetry (DSC) in a DSC 821 calorimeter from Mettler-Toledo (Schwerzenbach, Switzerland). Approximately, 6 mg of each material were placed into standard 40 mL aluminium crucibles and were subjected to a dynamic program under nitrogen atmosphere (flow rat 66 mL min^{-1}) divided in three steps: a first heating cycle from −50ºC up to 180ºC. This was followed by an isothermal stage at 180ºC for 2 min. Then, a cooling stage down to −50ºC was applied and, finally, a second heating stage up to 300ºC was scheduled. The heating and cooling rates for the all the scans were set to 10ºC min^{-1}. The melting temperature peak (T_m) and the degree of crystallinity (X_c) were obtained from the second heating cycle. The degree of crystallinity of PHB ($X_{c\ PHB}$) and PCL ($X_{c\ PCL}$) in each sample was determined using the following equation:

$$X_c\,(\%) = 100\ \times \left[\frac{\Delta H_m}{\Delta H_0 \cdot w}\right] \qquad \textbf{Equation 1}$$

Where ΔH_m stands for the thermodynamic melt enthalpy per gram of each polymer obtained from the second heating cycle, ΔH_0 is the theoretical enthalpy corresponding to the melting of a 100% crystalline PHB (146 J g^{-1} (Arrieta et al., 2014)) or PCL (156.8 J g^{-1} (Simoes et al., 2009)), and *w* is the weight fraction of the corresponding polymer (PHB or PCL) in the blend.

The thermal stability of unmodified and chemically modified HNT, as well as the PHB/PCL blends with HNT was studied by thermogravimetric analysis (TGA) in a TGA PT1000 from Linseis Inc. (Selb, Germany). Approximately 12 mg of each sample were subjected to a dynamic heating program from 30ºC up to 700ºC at a heating rate of 10ºC/min under nitrogen atmosphere with a constant flow rate of 66 mL min^{-1}. The onset degradation temperature (T_0) was defined as the temperature at which a 5% mass loss occurs. In addition, the maximum degradation temperature (T_{max}) for each stage was obtained as the corresponding peak of the first derivative (DTG).

2.5.6. Dynamic mechanical thermal analysis (DMTA)

Dynamic-mechanical thermal analysis (DMTA) was performed in an oscillatory rheometer AR G2 by TA Instruments (New Castle, USA) working in shear/torsion mode. This rheometer is equipped with a special clap system for solid samples thus allowing evaluation of dynamical-mechanical properties as a function of temperature. Samples with a size of 40x10x4 mm^3 were subjected to a temperature sweep from −100ºC up to 100ºC at a constant heating rate of 2ºC/min, a frequency of 1 Hz and a maximum shear strain (γ) of 0.1%. The values of storage modulus, G' and tan δ *versus* temperature were recorded for each sample. The glass transition temperature (T_g) was assumed as the peak maximum of the tan δ curve.

3. RESULTS AND DISCUSSION

3.1. Effect of chemical modification of HNT

The spectrum of unmodified HNT (Fig. 1) shows characteristic peaks located at 3695, 3624 and 912 cm^{-1} which are attributable to stretching of inner-surface Al−OH, the stretching of inner Al−OH and bending vibration of the inner Al−OH, respectively. The peaks located at 3450 and 1650 cm^{-1} are directly related to O–H stretching and bending vibration of the adsorbed water, respectively. Peaks centred at 1118, 1036 and 538 cm^{-1} are ascribed to the apical Si–O stretching vibration, in-plane Si–O stretching vibrations and Si−O bending vibration, respectively. It can also be detected the presence of two peaks at 792 cm^{-1} and 754 cm^{-1} which can be assigned to the symmetric stretching of Si−O−Si and the perpendicular stretching of Si−O−Al, respectively (Hillier et al., 2016; Pasbakhsh et al., 2010; Sun et al., 2015; Wang et al., 2013). The spectrum of the silanized HNT (HNT_{SIL}) (Fig. 1a) show a clear decrease in the absorbance of hydroxyl (–OH) groups in both internal and external layers related to peaks located at 3695, 3624 and 912 cm^{-1}. This can be explained by taking into account that silanol (Si–OH) groups obtained after the hydrolysis of the alkoxy groups in GLYMO, can react with hydroxyl groups of aluminol (Al–OH) in the inner layers of HNT as well as with the edges of the HNT and external surface defects on HNT. This decrease in the intensity of these peaks confirm the interaction of silane with HNT thus leading to formation of Al–O–Si bonds (Riza Erdogan et al., 2014). New absorption bands can be detected for the silanized HNT (HNT_{SIL}). It is worthy to note the peaks located at 2930 cm^{-1} and 2860 cm^{-1} which can be assigned to the asymmetric and symmetric stretching vibration of aliphatic $–CH_2$; the peak located at 1480 cm^{-1} is related to the deformation vibration of $–CH_2$ and corroborate the effectiveness of the silane treatment (Carli et al., 2014; Sun et al., 2016). Finally, the absorbance of the peaks related to the adsorbed water on HNT, located at 3450 cm^{-1} and 1650 cm^{-1} decreases after the silane treatment. This could be due to two overlapping phenomena: on one hand, this could be related to an increase in hydrophobicity after silanization, which restricts water adsorption. On the other hand, condensation reaction of silanol groups with aluminol groups leads to water generation that is removed after the drying process, thus contributing to a decrease on the overall amount of the adsorbed water between layers (Chow and

Neoh, 2009). With regard to caffeic acid modified HNT (HNT_{CA}) (Fig. 1b) shows the typical peaks ascribed to unmodified HNT but new peaks can identified. These peaks are located at 1646, 1622, 1452 and 1280 cm^{-1} and are related to C=C stretching, (-C=O) stretching of the -COOH group, the ring stretching and phenol (C-O) stretching from caffeic acid respectively (Williams et al., 2002). Furthermore, the peak related to the adsorbed water at 3450 cm^{-1} also decreases with regard to unmodified HNT, thus giving evidence of the hydrophobizing effect that caffeic acid can give on HNT.

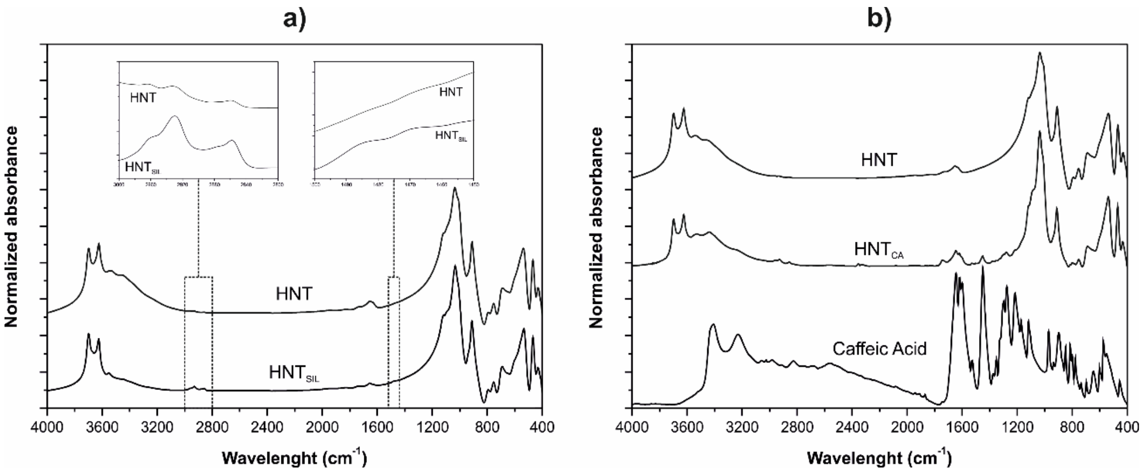

Fig. 1. FTIR spectra of unmodified HNT and, a) silanized HNT (HNT_{SIL}) with GLYMO and b) caffeic acid-loaded HNT (HNT_{CA}).

The effect of the different surface treatments on HNT was also followed by thermogravimetry (TGA) (Fig. 2). Unmodified HNT show two main mass loss steps. The first one is located in the temperature range comprised between 30 and 150ºC and is directly related to desorption of the water that is physically adsorbed onto HNT interlayers and surface and a second mass loss step located between 400–550ºC which is related to structural dehydroxylation of Al–OH groups of HNT (Garcia-Garcia et al., 2017a). After the silanization process, it is clearly distinguishable that the first mass loss step is smaller with regard to unmodified HNT. This is representative for the hydrophobizing properties the silane provides to HNT. Therefore, the amount of adsorbed water in the interlayer and surface is lower compared to unmodified HNT

(Carli et al., 2014). In addition, the overall mass loss on silanized HNT is slightly higher then unmodified HNT. This is due to thermal decomposition of organic compounds in GLYMO, grafted to HNT (Bischoff et al., 2015; Krishnaiah et al., 2017), thus giving evidence of the efficiency of the silanization process. With regard to the caffeic acid-loaded HNT, it can be also detected a decrease in the first mass loss step, thus indicating an increase in hydrophilic properties of HNT. The mass loss located in the 200–400ºC range is directly related to caffeic acid degradation. Caffeic acid decomposes in two main stages as reported in literature (Baykal et al., 2015). Regarding the mass loss in the 200–400ºC range, which represents a weight percentage of 28%, can be ascribed to removal of caffeic acid molecules chemically bonded to HNT or located into the lumen. Therefore, TGA analysis confirms the effectiveness of both silanized and caffeic acid-modified HNT.

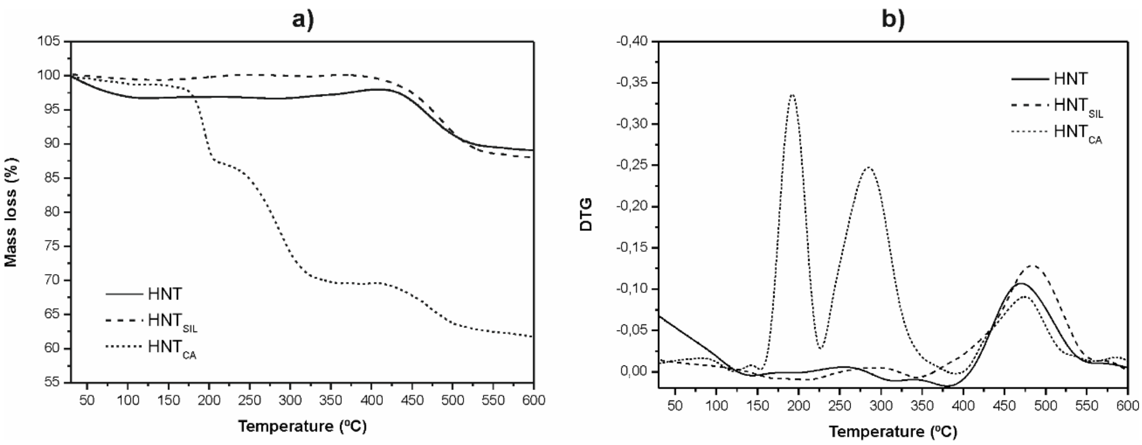

Fig. 2. a) TGA and b) DTGA of unmodified HNT and silanized HNT (HNT_{SIL}) with GLYMO and caffeic acid-loaded HNT (HNT_{CA}).

Morphological analysis using FESEM shows that HNT tend to form aggregates due to their intrinsic hydrophilic nature due to hydroxyl groups (Fig. 3a and b). These aggregates can reach a size of 50 μm, and this can negatively affect the overall performance of the PHB/PCL blend. After both silane and caffeic acid treatments, the hydrophobicity of HNT increases in a remarkable way due to the reaction of hydroxyl groups in HNT with GLYMO or caffeic acid which leads to formation of a thin hydrophobic layer that covers the external surface, Fig. 4. The hydrophobic effect of the silanes on the HNT has been demonstrated by several authors. Guo *et al.* (2009) and Zhang *et al.* (2013) improved the HNT hydrophobicity with 3-(trimethoxysilyl)propyl methacrylate. The same effect was observed by Haroosh *et al.* (2013) and Krishnaiah *et al.* (2017) after the HNT treatment with 3-aminopropyltriethoxysilane. Liu *et al.* (2008), Albdiry and Yousif (2013) and Bischoff *et al.* (2015) also showed as the HNT treatment with γ-glycidoxypropyltrimethoxysilane, vinyltrimethoxysilane and triethoxy(octyl)/trimethyl (octadecyl) silane, respectively, improved its hydrophobicity. One of the effects of hydrophobization is a remarkable decrease in the aggregate size, which is more evident in HNT loaded with caffeic acid (Fig. 3e and f). Table 2 contains the chemical composition of unmodified and chemically modified HNT by EDS. Silane treatment gives an increase in Si content with regard to unmodified HNT. After loading caffeic acid, the carbon content increases while both Al and Si content decrease which confirms the formation of a thin hydrophobic layer. So that, FESEM reveals the usefulness of both silane and caffeic acid treatments as the aggregate size is remarkable reduced and this has a positive effect on particle dispersion, which, in turn, will be able to improve the overall performance of the PHB/PCL blend.

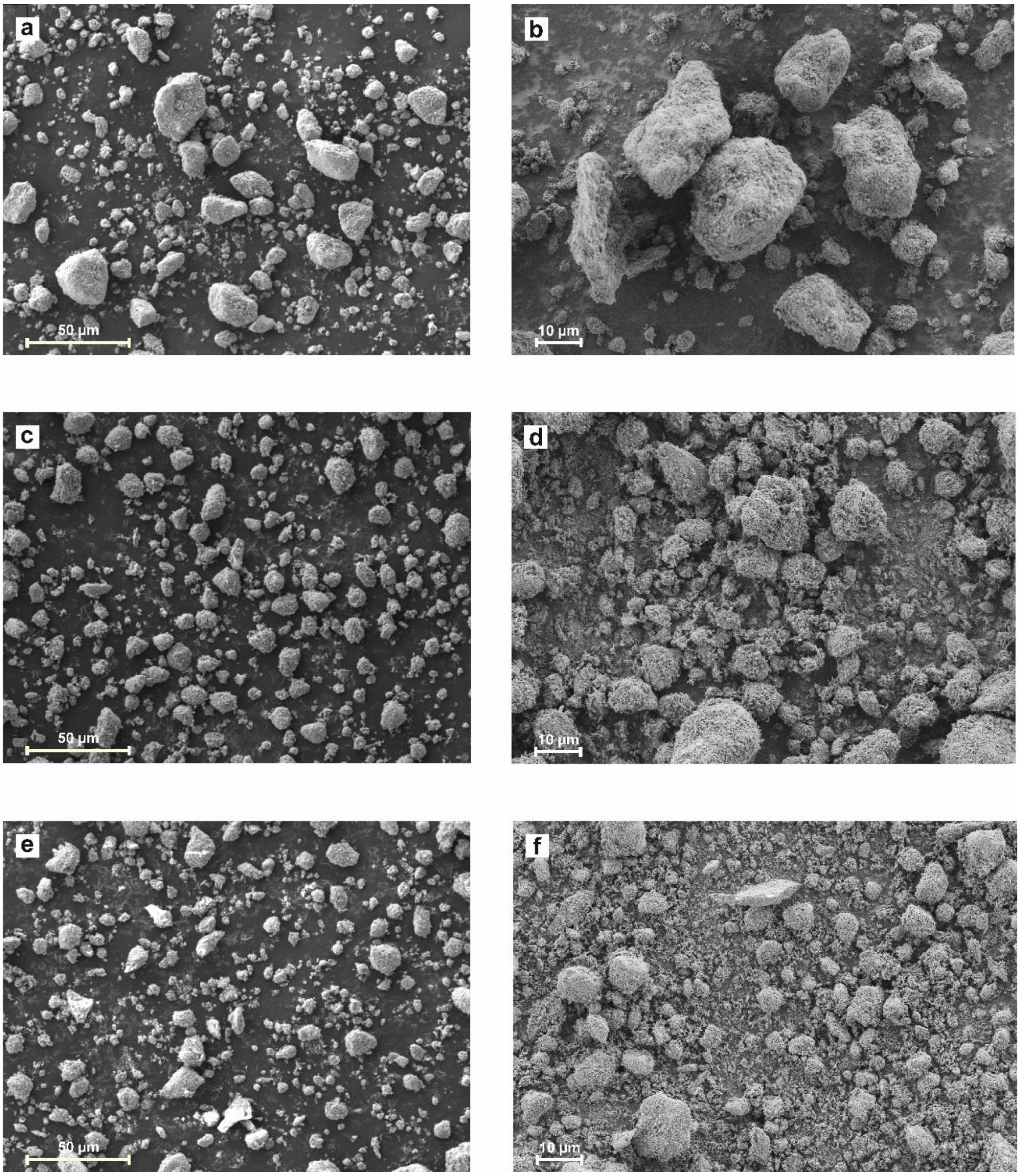

Fig. 3. FESEM images of a,b) unmodified HNT c,d) HNT modified with GLYMO silane (HNT_{SIL}) and e,f) HNT modified/loaded with caffeic acid (HNT_{CA}).

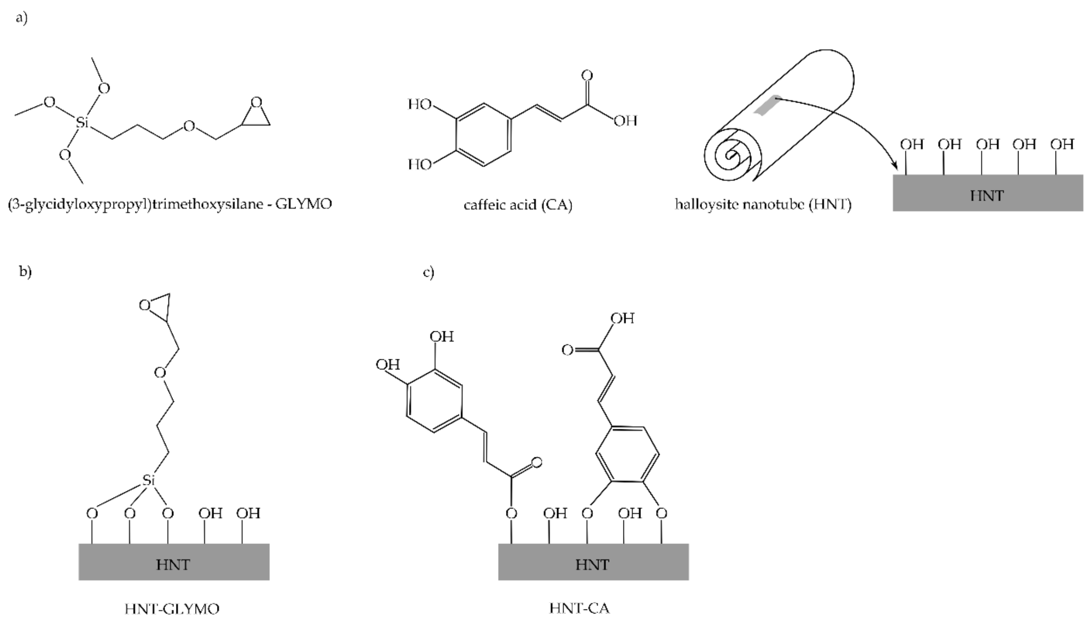

Fig. 4. a) Chemical structure of GLYMO, caffeic acid and HNT and schematic representation of the potential reaction of HNT with b) GLYMO and c) caffeic acid.

Samples	Element content (wt%)			
	C	O	Al	Si
HNT	2.5±0.8	50.9±4.2	23.7±2.1	22.9±1.8
HNT_{SIL}	2.1±0.2	50.9±0.9	23.1±0.8	23.9±0.9
HNT_{CA}	6.4±1.4	50.6±1.3	21.6±1.0	21.3±1.2

Table 2. Chemical composition of unmodified HNT, HNT modified with GLYMO silane (HNT_{SIL}) and HNT modified/loaded with caffeic acid (HNT_{CA}) obtained by EDS.

The increase in hydrophobicity was also studied by dynamic contact angle measurements, which is extremely sensitive to chemical changes in the surface (Fig. 5). The initial contact angle value (θ_0) for unmodified HNT is 120º but it quickly drops down to values around 0º (maximum hydrophilicity) after 15 s. This is a clear evidence of the hydrophilic nature of unmodified HNT. After both silane and caffeic acid treatments, hydrophobicity is remarkable improved. In both cases, the water drop remains with the same contact angle with very slight changes with time. Specifically, silanized HNT show an initial contact angle (θ_0) of 120º and drops down to a constant value of 100º that does not change with time. With regard to caffeic acid loaded HNT the hydrophobic behavior is still more accentuated. In fact, the initial contact angle at 0 s (θ_0) is 140º and decreases to a constant value of 120º, almost invariable with time.

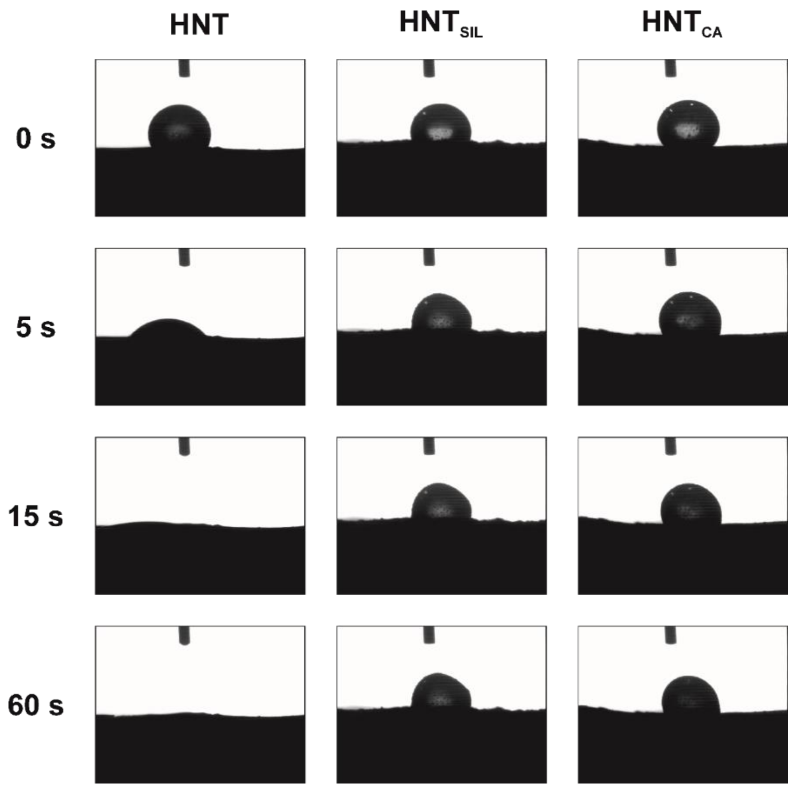

Fig. 5. Dynamic contact angle of water on a homogeneous layer of unmodified HNT, HNT with GLYMO silane (HNT_{SIL}) and caffeic acid modified/loaded (HNT_{CA}).

3.2. Characterization of PHB/PCL nanocomposites with HNT

3.2.1. Mechanical properties

Unloaded blend, shows a tensile strength of 22.2 MPa and an elastic modulus of 1324 MPa (Fig. 6). Regarding ductile properties, the use of reactive extrusion with 1 phr dicumyl peroxide (DCP) allows a remarkable improvement on elongation at break up to values of 21.8% which are similar to other previous results (Garcia-Garcia et al., 2017b). After the addition of 3 wt% HNT the blend becomes more brittle and a decrease in tensile strength down to 17.5 MPa and a remarkable decrease in elongation at break down to 11.2%. The elastic modulus, in contrast, remains almost constant with values of about 1315 MPa. This increase in brittleness is due to the presence of HNT aggregates in the matrix and the poor dispersion, which leads to a lack of continuity. HNT aggregates contribute to stress concentration with the subsequent embrittlement effect. Moreover, the highly hydrophilic nature of HNT is not compatible with the highly hydrophobic PHB/PCL blend, which also contributes to poor particle dispersion and stress concentration phenomena. Both silane and caffeic acid treatments increase hydrophobicity with a positive effect on particle dispersion as the aggregate size decreases in a remarkable way. This also allows an increase in compatibility between PHB and PCL which, in turn, will give improved mechanical performance regarding unmodified HNT (Garcia-Garcia et al., 2016). As it can be elucidated from the observation of Fig. 6a, PHB/PCL blend reinforced with 3 wt% of silanized and caffeic acid-loaded HNT show slightly increased tensile strength values of 19.8 MPa and 19.9 MPa respectively. In addition to an increase in mechanical resistant properties, the elongation at break is remarkably improved up to values of 15.8% and 19.5% for blends treated with silane and caffeic acid respectively. It is worthy to note the percentage increase in elongation at break that both silane and caffeic acid give to the base PHB/PCL blend which are 41 and 74% respectively. In a parallel way, the rigidity is reduced. In particular, the Young's modulus of the silanized and caffeic acid-loaded blend is 1282 MPa and 1224 MPa respectively. In general, it is possible to say that caffeic acid gives better properties to the base PHB/PCL blend with elongation at break values near the unreinforced blend values. This is mainly due to the hydrophobicity that caffeic acid provides to HNT which lead to smaller size aggregates and a better dispersion, all these having a positive effect on load transfer due to increased compatibility.

With regard to flexural properties, similar tendency can be observed (Fig. 6b). Addition of 3 wt% unmodified HNT leads to a decrease in the flexural strength of the PHB/PCL blend which changes from 39.3 MPa (unreinforced PHB/PCL blend) down to 32.4 MPa (PHB/PCL blend with 3 wt% unmodified HNT). The modulus is increased from 1151 MPa up to 1323 MPa (reinforced blend with unmodified HNT). Silanized HNT give better properties to the base

PHB/PCL blend with an increase in both the flexural strength and modulus up to 34.8 MPa and 1338 MPa respectively. Flexural properties of PHB/PCL blends containing 3 wt% caffeic acid-loaded HNT show similar flexural to composites with unmodified HNT but the flexural modulus is slightly lower, around 1196 MPa which indicates less rigidity.

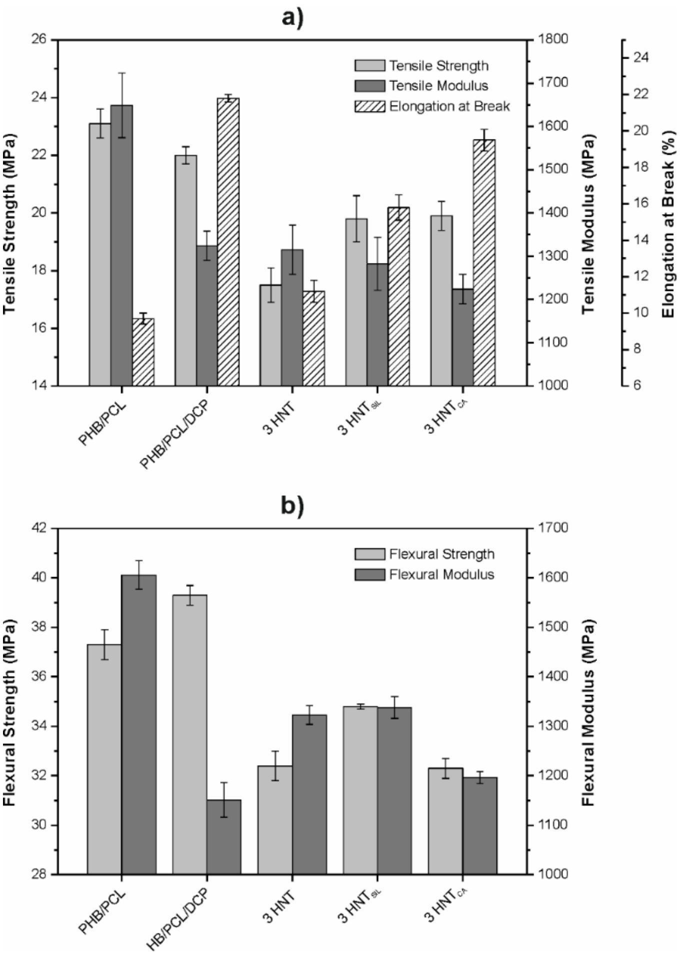

Fig. 6. a) Tensile properties and b) flexural properties of unreinforced PHB/PCL blend and PHB/PCL blend reinforced with 3 wt% of unmodified HNT, silanized HNT (HNT_{SIL}) and caffeic acid-loaded HNT (HNT_{CA}).

3.2.2. Thermal properties

The main thermal parameters of the base PHB/PCL blend and their composites with HNT were obtained by DSC and TGA (Table 3). As PHB and PCL are immiscible, two melt points are identified. The partially compatibilized PHB/PCL blend with reactive extrusion with DCP, shows two clear melt peak: one located at 54.4ºC which is attributed to the PCL rich phase and another one at 170.9ºC which is assigned to the PHB-rich phase. The effect of PCL is a slight decrease in both melt peak temperatures as reported in previous work, due to a slight increase in compatibility (Garcia-Garcia et al., 2017b). Addition of both unmodified and chemically-modified HNT does not affect in a remarkable way to the melt peak of the PCL-rich phase; nevertheless, the melt peak temperature corresponding to the PHB-rich phase decreases in a noticeable way. Regarding unmodified HNT, they provide a decrease in the characteristic melt peak of the PHB-rich phase of about 3ºC. This decrease is more evident for composites containing both silanized and caffeic acid-loaded HNT with characteristic peak values of 166.2ºC and 164.5ºC respectively. This decrease could be related with a better particle dispersion after the above mentioned treatments. Well dispersed HNT positively contribute to increase compatibility at the PHB/PCL interface which leads to a decrease in the peak temperature of neat PHB, and consequently, the PHB/PCL blend can be processed at lower temperatures. This feature is especially important for PHB-based blends as PHB shows poor thermal stability over its melt point. Caffeic acid-loaded HNT lead to a decrease in the melt peak of about 6.5ºC which expands the processing window of the blends, avoiding thermal degradation of PHB. The degree of crystallinity is also influenced by the presence of HNT (Table 3). The neat crystallinity of PCL is not highly affected after the addition of unmodified HNT and is maintained at levels of 26–28% for all blends with unmodified and chemically-modified HNT. Nevertheless, the effects of HNT on the overall crystallinity of the PHB-rich phase are more pronounced. As it can be outlined from **Table 3**, the PHB/PCL blend containing 3 wt% unmodified HNT slightly increase up to values around 50.7%. This could be due to the nucleant effect of HNT, despite this effect is restricted (Carli et al., 2011). Regarding PHB/PCL blends with chemically-modified HNT, it is worthy to note a remarkable decrease in the overall crystallinity down to values of 41.0% and 42.8% for silanized and caffeic acid-loaded HNT, respectively, due to a better particle dispersion over the matrix.

The thermal stability of PHB/PCL blends at high temperatures was studied by TGA (Table 3). These properties are the onset degradation temperature (T_0), the maximum degradation rate temperature for PCL ($T_{max\ PCL}$) and the maximum degradation rate temperature for the PHB-rich phase ($T_{max\ PHB}$) and were obtained from the corresponding TGA and DTG curves. All the developed materials show two main degradation steps related to PHB and PCL degradation respectively, which is also representative for poor miscibility. The unreinforced PHB/PCL blend shows a T_0 of 271.3ºC, a $T_{max\ PHB}$ of 288.4ºC and a $T_{max\ PCL}$ of 402.0ºC thus showing the exceptional thermal stability of PCL compared to PHB. As it can be observed, reactive extrusion with DCP improves the thermal stability of the PHB/PCL blend in a remarkable way due to an increase in miscibility (Garcia-Garcia et al., 2017b). Incorporation of HNT to the PHB/PCL blend does not affect in a remarkable extent to the thermal stability. Nevertheless, a slight increase (4ºC) in the onset degradation peak (T_0) can be detected after the addition of 3 wt% unmodified HNT. This thermal stabilization effect is more pronounced by using chemically-modified HNT reaching T_0 values of 277.8ºC and 276.4ºC for silanized and caffeic acid-loaded HNT, respectively. This slight increase can be due, as suggested by Du et al. (2006), to the fact that some volatile compounds generated in the initial degradation stages can be trapped inside the HNT lumen thus leading to a delay in the mass transfer with the subsequent increase in the thermal stability. Moreover, the better dispersion achieved with chemically-modified HNT results in higher randomness of lumen ends, thus leading to an increased effectiveness to trap some volatile degradation products. For this reason, PHB/PCL blend with chemically-modified HNT show improved thermal stability, measured through the T_0 value. It is also worthy top note that caffeic acid-loaded HNT offer a slightly lower T_0 compared to the silanized HNT. This could be due to the fact that the lumen in caffeic acid-loaded HNT is occupied by some caffeic acid molecules. With regard to the maximum degradation rate temperature of the PHB rich phase ($T_{max\ PHB}$), changes are negligible after addition of HNT, whatever their treatment. Nevertheless, a slight decrease in the thermal stability of the PCL-rich phase ($T_{max\ PCL}$) from 402ºC down to 395.3ºC and 395.8ºC for PHB/PCL blend with silanized and caffeic acid-loaded HNT, respectively, can be seen. This behaviour was reported by Çakman and Dilsiz (2016) and Terzopoulou et al. (2018).

Samples	DSC Parameters						TGA Parameters		
	$T_{m\ PCL}$ (ºC)	$\Delta H_{m\ PCL}$ (J g^{-1})	$X_{c\ PCL}$ (%)	$T_{m\ PHB}$ (ºC)	$\Delta H_{m\ PHB}$ (J g^{-1})	$X_{c\ PHB}$ (%)	T_0 (ºC)[a]	$T_{max\ PHB}$ (ºC)	$T_{max\ PCL}$ (ºC)
PHB/PCL/DCP	54.4	-44.7	28.5	170.9	-70.8	48.5	271.2	288.4	402.0
3-HNT	53.7	-43.6	27.8	168.1	-74.0	50.7	275.0	288.3	401.6
3-HNT_{SIL}	53.4	-40.6	25.9	166.2	-59.9	41.0	277.8	288.1	395.3
3-HNT_{AC}	53.6	-41.4	26.4	164.5	-62.5	42.8	276.4	288.4	395.8

[a] T_0, calculated at 5% mass loss.

Table 3. Thermal parameters of unreinforced PHB/PCL blend and PHB/PCL blend reinforced with 3 wt% of unmodified HNT, silanized HNT (HNT_{SIL}) and caffeic acid-loaded HNT (HNT_{CA}), obtained by differential scanning calorimetry (DSC) and thermogravimetric analysis (TGA).

3.2.3. Dynamic mechanical thermal analysis (DMTA)

As it can be deduced, the storage modulus (G') decreases with increasing temperature due to an increase in chain mobility with temperature (Fig. 7). In addition, two relaxation processes can be clearly identified, which is also representative for low miscibility between PHB and PCL. G' increases after addition of HNT to the PHB/PCL base blend (Fig. 7a). This difference is much pronounced in the rubbery state which is located between the glass transition temperature of both polymers (−52.6ºC and 9.8ºC) (Garcia-Garcia et al., 2016). This increase in G' is due to HNT since these nanoparticles provide a high level of mechanical restriction thus, reducing chain mobility and overall deformation ability, with the subsequent embrittlement. Unmodified and silanized HNT give the highest G' values which is representative for poor interactions between HNT and the surrounding matrix. This lack of compatibility gives poor material cohesion and leads to fracture with low deformation. With regard to caffeic acid-loaded HNT, they contribute to lower the G' values which is a clear evidence of somewhat interactions between HNT and the PHB/PCL blend.

The glass transition temperature (T_g) was obtained and analysed through the peak values of the damping factor (tan δ) (Fig. 7b). Two clear peaks are observed for all samples which give evidence of immiscibility. After that addition of HNT the T_g of the PHB-rich phase is not highly affected and is maintained at values of 9–10ºC for all samples independently of the surface treatment on HNT. Nevertheless, the T_g of the PCL-rich phase is more affected by the presence of HNT, especially chemically-modified HNT. In fact, the initial T_g of the PCL-rich phase in unfilled PHB/PCL blend is −52.6 ºC and it still decreased down to values of −63.0ºC and −62.2ºC in blends with silanized and caffeic acid-loaded HNT, respectively. This is not the expected behaviour since HNT contribute to restricted chain mobility with the subsequent increase in T_g (Liu et al., 2013). This unexpected behaviour could be related to the plasticization effect of the surfactants in HNT (Zhao et al., 2013) together with an increase in the amorphous volume fraction due to the addition of the HNT (Pasbakhsh et al., 2010).

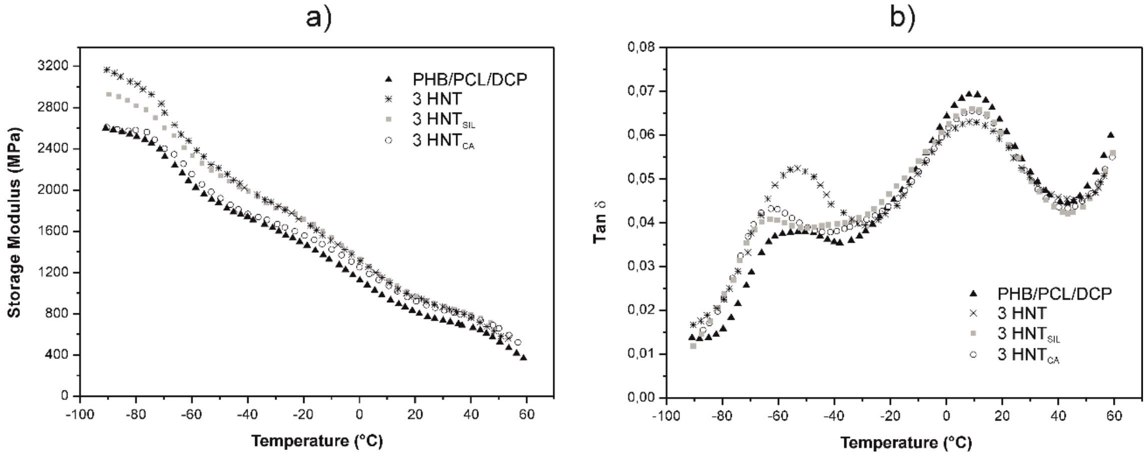

Fig. 7. Dynamic mechanical thermal analysis (DMTA) curves a) storage modulus, G' and b) damping factor (tan δ) of unreinforced PHB/PCL blend and PHB/PCL blend reinforced with 3 wt% of unmodified HNT, silanized HNT (HNT_{SIL}) and caffeic acid-loaded HNT (HNT_{CA}).

3.2.4. Surface Morphology study

FESEM images of the fractured surfaces from impact tests of PHB/PCL blend without and with HNT with different surface treatments show how all samples exhibit a homogeneous fracture surface without the typical phase separation (drop-like) structure in immiscible polymer blends (Fig. 8). It is important to remark that the base PHB/PCL formulation was obtained through reactive extrusion with DCP (Garcia-Garcia et al., 2017b). FESEM images also reveal presence of some HNT in the fracture surface. The sample with 3 wt% unmodified HNT shows lack of continuity due to presence of large size aggregates (Fig. 8c and d). This absence of continuity is produced by the lack of interactions between the highly hydrophilic HNT and the highly hydrophobic surround matrix. This is reflected in FESEM images by the presence of a small gap between the HNT aggregates and the surrounding matrix with a negative effect on overall mechanical properties as described previously. In fact, this lack of interaction is responsible for a stress concentration phenomenon which leads to reduced elongation due to poor material cohesion. This gap is not detectable for composites containing both silanized and caffeic acid-loaded HNT due to the increase in hydrophobicity these two treatments provide to HNT which, in turn, positively contribute to particle dispersion and, subsequently, to improved mechanical properties (Fig. 8e-h). Surface treatments on HNT do not only provide better dispersion but also small aggregate size which provide more cohesion to the material. The better dispersion of HNT can be observed through the elemental mapping of carbon, oxygen and silicon (Fig. 9).

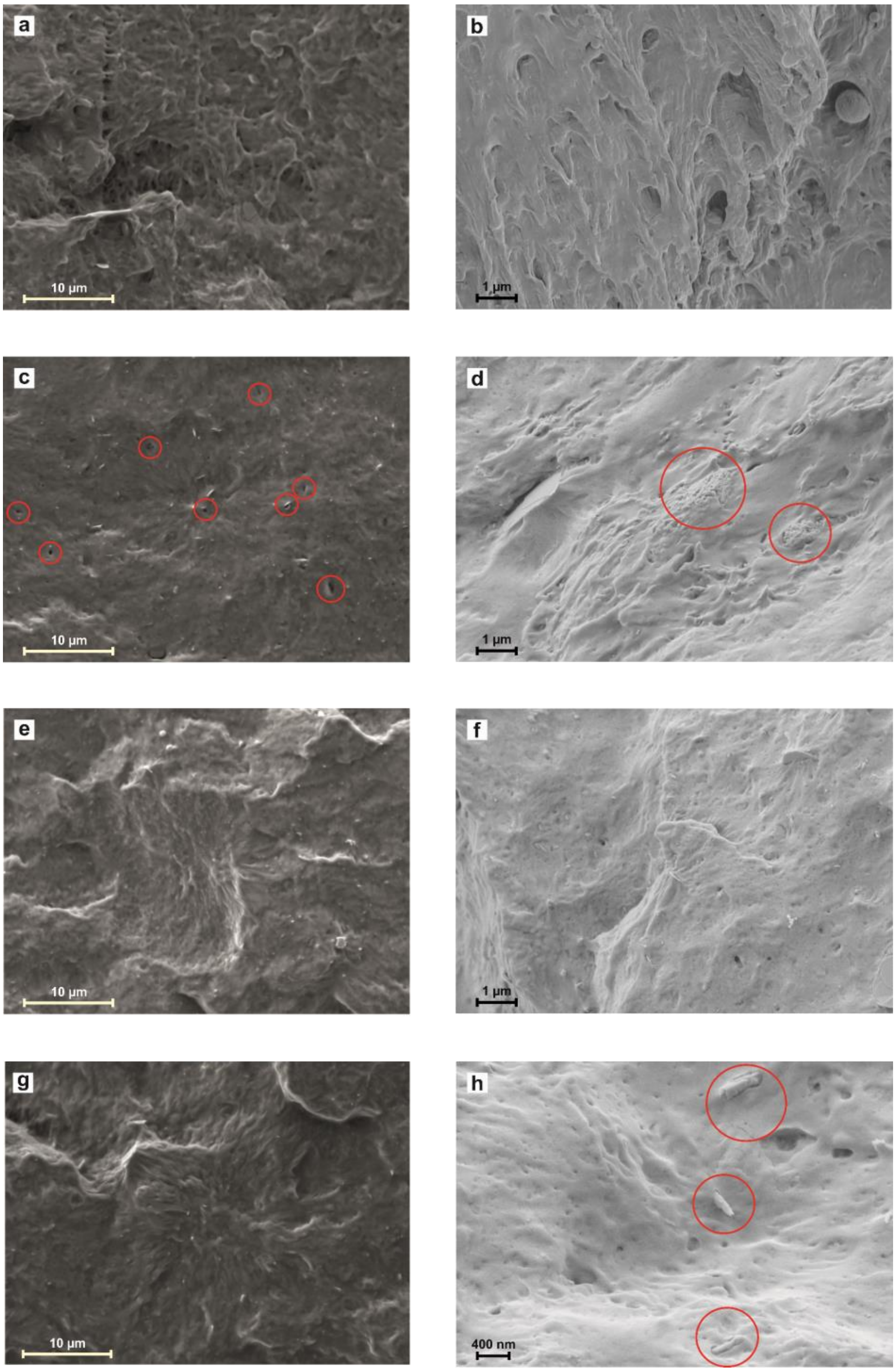

Fig. 8. FESEM images of impact-fractured surfaces of PHB/PCL blend partially compatibilized by reactive extrusion with dicumyl peroxide (DCP) and 3 wt% HNT: a,b) PHB/PCL/DCP, c,d) unmodified HNT, e,f) silanized (GLYMO) HNT (HNT_{SIL}) and g,h) caffeic acid-loaded HNT (HNT_{CA}).

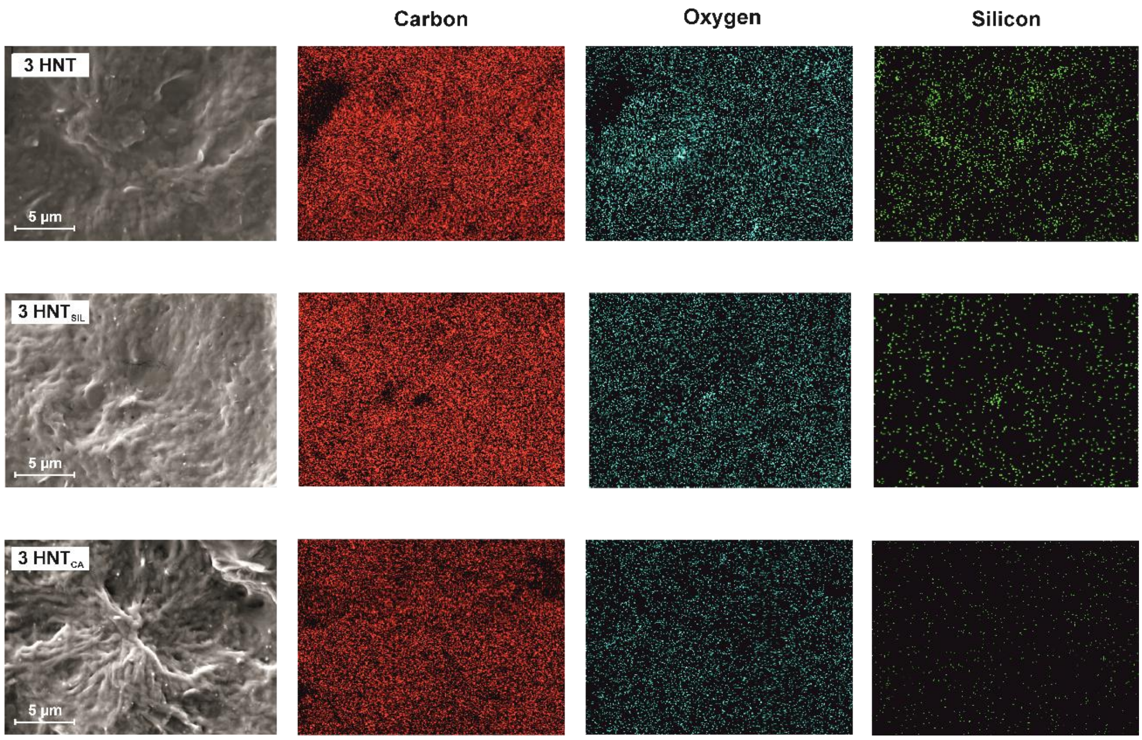

Fig. 9. Elemental mapping of carbon, oxygen and silicon of impact-fractured surfaces of PHB/PCL blend partially compatibilized by reactive extrusion with dicumyl peroxide (DCP) and 3 wt% HNT: a) unmodified HNT, b) silanized (GLYMO) HNT (HNT$_{SIL}$) and c) caffeic acid-loaded HNT (HNT$_{CA}$).

4. CONCLUSIONS

Unmodified and chemically-modified (silanized and caffeic acid-loaded) halloysite nanotubes (HNT) were successfully incorporated into PHB/PCL blends partially compatibilized by reactive extrusion with 1 phr dicumyl peroxide (DCP) and subsequent injection molding. Both silanization with 3-glycidyloxypropyl trimethoxysilane and caffeic acid treatment, led to increased hydrophobicity in HNT, which was particularly improved by the caffeic acid loading treatment. This increase in hydrophobicity had a positive effect on avoiding aggregate formation thus leading to a better particle dispersion as confirmed by FESEM-EDS. Mechanical characterization showed a remarkable increase in both mechanical resistant properties (tensile strength) and ductile properties (elongation at break) by using chemically-modified HNT compared to unmodified HNT. These results suggests the silanized and caffeic acid-loaded HNT contribute to improve interactions with the polymer matrix since the high hydrophilic nature of unmodified HNT does not allow good particle dispersion. In addition, it is worthy to note that PHB-based materials are high sensitive to thermal degradation as PHB degrades quickly over its melt point. Both chemically-modified HNT lead to a decrease in the melt peak temperature of the PHB-rich phase (of about 5−6ºC) together with a delay of 5−6ºC in the onset degradation temperature. Therefore, the processing window is extended by 10ºC to 12ºC which is an important issue for PHB-based materials. As an overall conclusion, it is worthy to note the interesting properties that caffeic acid-loaded HNT can give to PHB/PCL blend in terms of mechanical properties and thermal behaviour.

ACKNOWLEDGEMENTS

This work was supported by the Ministry of Economy and Competitiveness (MINECO) [MAT2017-84909-C2-2-R]. D. Garcia-Garcia wants to thank the Spanish Ministry of Education, Culture and Sports for the financial support through a FPU grant [FPU13/06011].

REFERENCES

Albdiry, M.T., Yousif, B.F., 2013. Morphological structures and tribological performance of unsaturated polyester based untreated/silane-treated halloysite nanotubes. Mater. Des. 48, 68-76.

Arrieta, M.P., Samper, M.D., López, J., Jiménez, A., 2014. Combined effect of poly (hydroxybutyrate) and plasticizers on polylactic acid properties for film intended for food packaging. J. Polym. Environ. 22, 460-470.

Azuma, Y., Yoshie, N., Sakurai, M., Inoue, Y., Chûjô, R., 1992. Thermal behaviour and miscibility of poly (3-hydroxybutyrate)/poly (vinyl alcohol) blends. Polymer. 33, 4763-4767.

Baykal, A., Amir, M., Günerb, S., Sözeri, H., 2015. Preparation and characterization of SPION functionalized via caffeic acid. J. Magn. Magn. Mater. 395, 199-204.

Bischoff, E., Daitx, T., Simon, D.A., Schrekker, H.S., Liberman, S.A., Mauler, R.S., 2015. Organosilane-functionalized halloysite for high performance halloysite/heterophasic ethylene–propylene copolymer nanocomposites. Appl. Clay Sci. 112, 68-74.

Çakman, G., Dilsiz, N., 2016. Preparation and Physical, Thermal Properties of Polycaprolactone/m-Halloysite Nanocomposite. Journal of Multidisciplinary Engineering Science Studies. 2, 842-848.

Carli, L.N., Crespo, J.S., Mauler, R.S., 2011. PHBV nanocomposites based on organomodified montmorillonite and halloysite: the effect of clay type on the morphology and thermal and mechanical properties. Composites, Part A. 42, 1601-1608.

Carli, L.N., Daitx, T.S., Soares, G.V., Crespo, J.S., Mauler, R.S., 2014. The effects of silane coupling agents on the properties of PHBV/halloysite nanocomposites. Appl. Clay Sci. 87, 311-319.

Chen, R.S., Ahmad, S., Gan, S., Ghani, A., Hafizuddin, M., Salleh, M.N., 2015. Effects of compatibilizer, compounding method, extrusion parameters, and nanofiller loading in clay-reinforced recycled HDPE/PET nanocomposites. J. Appl. Polym. Sci. 132, 42287.

Choi, J.S., Park, W.H., 2004. Effect of biodegradable plasticizers on thermal and mechanical properties of poly (3-hydroxybutyrate). Polym. Test. 23, 455-460.

Chow, W., Neoh, S., 2009. Dynamic mechanical, thermal, and morphological properties of silane-treated montmorillonite reinforced polycarbonate nanocomposites. J. Appl. Polym. Sci. 114, 3967-3975.

Díez-Pascual, A.M., Díez-Vicente, A.L., 2014. Poly (3-hydroxybutyrate)/ZnO bionanocomposites with improved mechanical, barrier and antibacterial properties. Int. J. Mol. Sci. 15, 10950-10973.

Du, M., Guo, B., Jia, D., 2006. Thermal stability and flame retardant effects of halloysite nanotubes on poly (propylene). Eur. Polym. J. 42, 1362-1369.

Garcia-Garcia, D., Ferri, J., Boronat, T., López-Martínez, J., Balart, R., 2016. Processing and characterization of binary poly (hydroxybutyrate)(PHB) and poly (caprolactone)(PCL) blends with improved impact properties. Polym. Bull. 73, 3333-3350.

Garcia-Garcia, D., Ferri, J.M., Ripoll, L., Hidalgo, M., Lopez-Martinez, J., Balart, R., 2017a. Characterization of selectively etched halloysite nanotubes by acid treatment. Appl. Surf. Sci. 422, 616-625.

Garcia-Garcia, D., Rayón, E., Carbonell-Verdu, A., Lopez-Martinez, J., Balart, R., 2017b. Improvement of the compatibility between poly (3-hydroxybutyrate) and poly (ε-caprolactone) by reactive extrusion with dicumyl peroxide. Eur. Polym. J. 86, 41-57.

Garcia-Garcia, D., Carbonell-Verdu, A., Jordá-Vilaplana, A., Balart, R., Garcia-Sanoguera, D., 2016. Development and characterization of green composites from bio-based polyethylene and peanut shell. J. Appl. Polym. Sci. 133.

Garcia-Garcia, D., Fenollar, O., Fombuena, V., Lopez-Martinez, J., Balart, R., 2017. Improvement of mechanical ductile properties of poly (3-hydroxybutyrate) by using vegetable oil derivatives. Macromol. Mater. Eng. 302, 1600330.

Gassner, F., Owen, A., 1994. Physical properties of poly (β-hydroxybutyrate)-poly (ε-caprolactone) blends. Polymer. 35, 2233-2236.

Godbole, S., Gote, S., Latkar, M., Chakrabarti, T., 2003. Preparation and characterization of biodegradable poly-3-hydroxybutyrate–starch blend films. Bioresour. Technol. 86, 33-37.

Guo, B., Zou, Q., Lei, Y., Jia, D., 2009. Structure and performance of polyamide 6/halloysite nanotubes nanocomposites. Polym. J. 41, 835-842.

Haroosh, H.J., Dong, Y., Chaudhary, D.S., Ingram, G.D., Yusa, S., 2013. Electrospun PLA: PCL composites embedded with unmodified and 3-aminopropyltriethoxysilane (ASP) modified halloysite nanotubes (HNT). Appl. Phys. A: Mater. Sci. Process. 110, 433-442.

Hemmati, F., Garmabi, H., Modarress, H., 2014. Effects of organoclay on the compatibility and interfacial phenomena of PE/EVA blends with UCST phase behavior. Polym. Compos. 35, 2329-2342.

Hendessi, S., Sevinis, E.B., Unal, S., Cebeci, F.C., Menceloglu, Y.Z., Unal, H., 2016. Antibacterial sustained-release coatings from halloysite nanotubes/waterborne polyurethanes. Prog. Org. Coat. 101, 253-261.

Hillier, S., Brydson, R., Delbos, E., Fraser, T., Gray, N., Pendlowski, H., Phillips, I., Robertson, J., Wilson, I., 2016. Correlations among the mineralogical and physical properties of halloysite nanotubes (HNTs). Clay Miner. 51, 325-350.

Iulianelli, G.C.V., David, G.d.S., dos Santos, T.N., Sebastião, P.J.O., Tavares, M.I.B., 2018. Influence of TiO 2 nanoparticle on the thermal, morphological and molecular characteristics of PHB matrix. Polym. Test. 65, 156-162.

Jafarzadeh, S., Haddadi-Asl, V., Roghani-Mamaqani, H., 2015. Nanofibers of poly (hydroxyethyl methacrylate)-grafted halloysite nanotubes and polycaprolactone by combination of RAFT polymerization and electrospinning. J. Polym. Res. 22, 123.

Krishnaiah, P., Ratnam, C.T., Manickam, S., 2017. Development of silane grafted halloysite nanotube reinforced polylactide nanocomposites for the enhancement of mechanical, thermal and dynamic-mechanical properties. Appl. Clay Sci. 135, 583-595.

Kurczewska, J., Cegłowski, M., Messyasz, B., Schroeder, G., 2018. Dendrimer-functionalized halloysite nanotubes for effective drug delivery. Appl. Clay Sci. 153, 134-143.

Kurusu, R.S., Demarquette, N.R., Gauthier, C., Chenal, J.M., 2014. Effect of ageing and annealing on the mechanical behaviour and biodegradability of a poly (3-hydroxybutyrate) and poly (ethylene-co-methyl-acrylate-co-glycidyl-methacrylate) blend. Polym. Int. 63, 1085-1093.

Liu, M., Guo, B., Du, M., Lei, Y., Jia, D., 2008. Natural inorganic nanotubes reinforced epoxy resin nanocomposites. J. Polym. Res. 15, 205-212.

Liu, M., Zhang, Y., Zhou, C., 2013. Nanocomposites of halloysite and polylactide. Appl. Clay Sci. 75, 52-59.

Lovera, D., Márquez, L., Balsamo, V., Taddei, A., Castelli, C., Müller, A.J., 2007. Crystallization, morphology, and enzymatic degradation of polyhydroxybutyrate/polycaprolactone (PHB/PCL) blends. Macromol. Chem. Phys. 208, 924-937.

Lvov, Y.M., Shchukin, D.G., Mohwald, H., Price, R.R., 2008. Halloysite clay nanotubes for controlled release of protective agents. ACS Nano. 2, 814-820.

Ma, P., Hristova-Bogaerds, D.G., Lemstra, P.J., Zhang, Y., Wang, S., 2012. Toughening of PHBV/PBS and PHB/PBS Blends via In situ Compatibilization Using Dicumyl Peroxide as a Free-Radical Grafting Initiator. Macromol. Mater. Eng. 297, 402-410.

Mofokeng, J.P., Luyt, A.S., 2015. Dynamic mechanical properties of PLA/PHBV, PLA/PCL, PHBV/PCL blends and their nanocomposites with TiO 2 as nanofiller. Thermochim. Acta. 613, 41-53.

Olkhov, A., Vlasov, S., Iordanskii, A., Zaikov, G., Lobo, V., 2003. Water transport, structure features and mechanical behavior of biodegradable PHB/PVA blends. J. Appl. Polym. Sci. 90, 1471-1476.

Pal, P., Kundu, M.K., Malas, A., Das, C.K., 2014. Compatibilizing effect of halloysite nanotubes in polar–nonpolar hybrid system. J. Appl. Polym. Sci. 131, 39587.

Pasbakhsh, P., Ismail, H., Fauzi, M.A., Bakar, A.A., 2010. EPDM/modified halloysite nanocomposites. Appl. Clay Sci. 48, 405-413.

Raman, V., Rooj, S., Das, A., Stöckelhuber, K., Simon, F., Nando, G., Heinrich, G., 2013. Reinforcement of solution styrene butadiene rubber by silane functionalized halloysite nanotubes. J. Macromol. Sci., Part A: Pure Appl.Chem. 50, 1091-1106.

Riza Erdogan, A., Kaygusuz, I., Kaynak, C., 2014. Influences of aminosilanization of halloysite nanotubes on the mechanical properties of polyamide-6 nanocomposites. Polym. Compos. 35, 1350-1361.

S de O Patrício, P., Pereira, F.V., dos Santos, M.C., de Souza, P.P., Roa, J.P., Orefice, R.L., 2013. Increasing the elongation at break of polyhydroxybutyrate biopolymer: Effect of cellulose nanowhiskers on mechanical and thermal properties. J. Appl. Polym. Sci. 127, 3613-3621.

Simoes, C., Viana, J., Cunha, A., 2009. Mechanical properties of poly(ε-caprolactone) and poly (lactic acid) blends. J. Appl. Polym. Sci. 112, 345-352.

Sun, P., Liu, G., Lv, D., Dong, X., Wu, J., Wang, D., 2015. Effective activation of halloysite nanotubes by piranha solution for amine modification via silane coupling chemistry. RSC Adv. 5, 52916-52925.

Sun, P., Liu, G., Lv, D., Dong, X., Wu, J., Wang, D., 2016. Simultaneous improvement in strength, toughness, and thermal stability of epoxy/halloysite nanotubes composites by interfacial modification. J. Appl. Polym. Sci. 133, 43249.

Taguet, A., Cassagnau, P., Lopez-Cuesta, J.-M., 2014. Structuration, selective dispersion and compatibilizing effect of (nano) fillers in polymer blends. Prog. Polym. Sci. 39, 1526-1563.

Terzopoulou, Z., Papageorgiou, D.G., Papageorgiou, G.Z., Bikiaris, D.N., 2018. Effect of surface functionalization of halloysite nanotubes on synthesis and thermal properties of poly(ε-caprolactone). J. Mater. Sci. 53, 6519-6541.

Torres, E., Fombuena, V., Vallés-Lluch, A., Ellingham, T., 2017. Improvement of mechanical and biological properties of Polycaprolactone loaded with Hydroxyapatite and Halloysite nanotubes. Mater. Sci. Eng., C. 75, 418-424.

Urquijo, J., Aranburu, N., Dagréou, S., Guerrica-Echevarría, G., Eguiazábal, J., 2017. CNT-induced morphology and its effect on properties in PLA/PBAT-based nanocomposites. Eur. Polym. J. 93, 545-555.

Vrsaljko, D., Macut, D., Kovačević, V., 2015. Potential role of nanofillers as compatibilizers in immiscible PLA/LDPE blends. J. Appl. Polym. Sci. 132, 41414.

Wang, Q., Zhang, J., Wang, A., 2013. Alkali activation of halloysite for adsorption and release of ofloxacin. Appl. Surf. Sci. 287, 54-61.

Williams, P.A., Baro, A.G., Ferrer, E.G., 2002. Study of the interaction of oxovanadium (IV) with a plant component (caffeic acid). Synthesis and characterization of a solid compound. Polyhedron. 21, 1979-1984.

Wu, D., Lin, D., Zhang, J., Zhou, W., Zhang, M., Zhang, Y., Wang, D., Lin, B., 2011. Selective localization of nanofillers: effect on morphology and crystallization of PLA/PCL blends. Macromol. Chem. Phys. 212, 613-626.

Yuan, P., Southon, P.D., Liu, Z., Green, M.E., Hook, J.M., Antill, S.J., Kepert, C.J., 2008. Functionalization of halloysite clay nanotubes by grafting with γ-aminopropyltriethoxysilane. J. Phys. Chem.: C. 112, 15742-15751.

Zhang, J., Zhang, D., Zhang, A., Jia, Z., Jia, D., 2013. Poly (methyl methacrylate) grafted halloysite nanotubes and its epoxy acrylate composites by ultraviolet curing method. J. Reinf. Plast. Compos. 32, 713-725.

Zhang, M., Thomas, N.L., 2010. Preparation and properties of polyhydroxybutyrate blended with different types of starch. J. Appl. Polym. Sci. 116, 688-694.

Zhang, M., Thomas, N.L., 2011. Blending polylactic acid with polyhydroxybutyrate: the effect on thermal, mechanical, and biodegradation properties. Adv. Polym. Technol. 30, 67-79.

Zhao, H., Cui, Z., Wang, X., Turng, L.-S., Peng, X., 2013. Processing and characterization of solid and microcellular poly (lactic acid)/polyhydroxybutyrate-valerate (PLA/PHBV) blends and PLA/PHBV/Clay nanocomposites. Composites, Part B. 51, 79-91.